Compound-Specific and Intramolecular $\delta^{15}N$ analysis of a Poly-Nitrogenous Amino Acid: Histidine.

Charlotte Wing Man Lee[1†], Mark A. Altabet[2], Jesus Baca[1], Jason Barrera[1], and Lin Zhang[1*]

(1) Texas A&M University Corpus Christi, Corpus Christi, TX, United States,

(2) University of Massachusetts Dartmouth, School for Marine Science and Technology, New Bedford, MA, United States

* Corresponding Author: Lin Zhang (lin.zhang@tamucc.edu)

†Present Addresses: Woods Hole Oceanographic Institution, MA, United States

Abstract

Histidine (HIS) is an essential amino acid (AA) with key physiological roles in metal chelation and proton buffering. Its three nitrogen (N) atoms—one α-amino and two in the imidazole side chain—are incorporated through distinct biosynthetic pathways and undergo different catabolic processes. Thus, its intramolecular $\delta^{15}N$ likely provides additional information on these pathways and associated N fluxes. Very few studies have reported molecular average $\delta^{15}N_{HIS}$ ($\delta^{15}N_{HIS\text{-}Total}$) and there are no reported intramolecular $\delta^{15}N_{HIS}$ data for natural materials due to the technical limitations of available methods. Here, we present a novel analytical approach for compound-specific and intramolecular $\delta^{15}N$ of poly-nitrogenous AAs using HIS as an example, such analytical scheme can be adapted to obtain position-specific $\delta^{15}N$ of other key AAs with two N atoms such as glutamine. Underivatized HIS is separated by ion-exchange chromatography (IC) and divided into two aliquots. One fraction is fully oxidized to NO_3^- using UV-persulfate oxidation for $\delta^{15}N_{HIS\text{-}Total}$ measurement, while the other undergoes NaClO oxidation, selectively converting α-N and a minor fraction of sidechain-N to NO_2^- at a known ratio. $\delta^{15}N_{HIS}$ of α-N ($\delta^{15}N_{HIS\text{-}\alpha}$) and sidechain-N ($\delta^{15}N_{HIS\text{-}s}$) are then calculated from these two results. Our findings reveal that α-N is consistently enriched in ^{15}N relative to sidechain-N in both commercial HIS powder ($\Delta\delta^{15}N_{\alpha\text{-}s}$ = ~ + 8‰) and biological samples ($\Delta\delta^{15}N_{\alpha\text{-}s}$ = ~ + 3 to 25‰), likely due to preferential α-N catabolism via deamination. This finding supports the potential of studying diverse biosynthetic and catabolic processes of poly-nitrogenous AAs using intramolecular $\delta^{15}N$.

1. Introduction

Nitrogen (N) isotopic composition ($\delta^{15}N$) of amino acids (AAs) has been widely applied to study N assimilation, biosynthesis, and metabolism, as well as trophic dynamics in ecosystems[1-6]. The interpretative power of this tool stems from the N isotopic fractionation induced by biochemical reactions involving the breakage or formation of C-N bonds, mostly driven by transamination and deamination of the α-N[7, 8]. However, the intramolecular ^{15}N distribution within poly-nitrogenous AAs, where sidechain N atoms may experience different biochemical reactions compared to the α-N, remains largely unexplored.

Histidine (HIS) is a structurally unique essential amino acid containing three nitrogen atoms—one α-N and two in the imidazole sidechain. Beyond its role in protein synthesis, HIS functions as a proton buffer, a metal ion chelator, and a catalytic site in metalloenzymes[9-12]. It also serves as a precursor to biologically important compounds such as urocanic acid, carnosine, and N-acetyl-histidine, which are critical for vertebrate growth and metabolism[13 14, 15]. HIS $\delta^{15}N$ values ($\delta^{15}N_{HIS}$) could thus be a useful tool to study the biosynthesis and metabolism of HIS and the factors regulating these processes.

During HIS biosynthesis in primary producers, the α-N is derived from glutamic acid via transamination, while the imidazole N atoms originate from glutamine and ATP[16, 17](Supplementary Figure 1a). Unlike AAs such as glutamic acid, aspartic acid, valine, alanine, leucine, and isoleucine, which readily exchange N with each other and with cellular ammonia—collectively termed the "metabolic N pool"[18]—HIS does not undergo significant N exchange in vivo, as demonstrated by isotope-labeling experiments[19, 20]. As a result, the molecular average $\delta^{15}N$ value of HIS ($\delta^{15}N_{HIS\text{-}Total}$) may be decoupled from the isotopic composition of AAs that participate extensively in transamination, such as glutamic acid (Glu), which is typically significantly enriched in ^{15}N due to its role in N metabolism [18]. This distinction is evident in marine organisms and human hair, where $\delta^{15}N_{HIS\text{-}Total}$ is consistently lower than $\delta^{15}N$ of Glu by more than 10‰[21-24]. During the synthesis of non-essential AAs, transamination progressively increases ^{15}N enrichment in the metabolic N pool, a trend that becomes more pronounced at higher trophic levels. However, since HIS does not interact significantly with this pool, its $\delta^{15}N$ does not increase substantially with trophic transfer. Given the high biosynthetic cost of HIS (~41 ATP)[16, 25], organisms may preferentially incorporate dietary HIS rather than degrade it, potentially preserving the original $\delta^{15}N$ signature of the dietary HIS[26]. Consequently, $\delta^{15}N_{HIS\text{-}Total}$ may serve as an indicator of the $\delta^{15}N$ composition of the basal N source within an ecosystem[18].

In addition to $\delta^{15}N_{HIS\text{-}Total}$, intramolecular $\delta^{15}N_{HIS}$ could provide insight into biosynthetic pathways and corresponding isotope fractionation that each N atom experiences. The α-N can be catabolized via irreversible deamination by histidine ammonia-lyase (Supplementary Figure 1b), whereas complete degradation pathways for the imidazole ring are absent in many lower eukaryotes and plants[27, 28]. Compared to the sidechain-N atoms, the α-N atom is more likely subjected to HIS catabolism that irreversibly cleaves the C-N bond and thus induces isotopic fractionation to the α-N atom ($\delta^{15}N_{HIS\text{-}\alpha}$). Thus, the two N atoms in the imidazole ring might preserve the original isotopic composition of HIS imprinted from the biosynthesis by primary producers with minimal alteration. As a result, the $\delta^{15}N$ of sidechain N ($\delta^{15}N_{HIS\text{-}s}$) may retain the original biosynthetic isotope signals, while $\delta^{15}N_{HIS\text{-}\alpha}$ may reflect the isotopic fractionation through deamination, which is not directly related to the ^{15}N enrichment in the metabolic N pool caused by transamination. These differences could provide insights into physiological and nutritional status, independent of trophic fractionation effects.

Despite its potential, $\delta^{15}N_{HIS}$ measurements have been limited by analytical challenges. Traditional $\delta^{15}N_{HIS}$ analysis using gas chromatography-combustion-isotope ratio mass spectrometry (GC/C/IRMS) requires derivatization. Common HIS derivatives exhibit low recovery, long retention times, and frequent coelution with other AAs[20, 29-34]. The imidazole group may lead to incomplete reactions and formation of N-containing side products that are lost during preparation, as the common derivative reagents also react with the imidazole-N[35, 36]. The only reported attempt to measure intramolecular $\delta^{15}N_{HIS}$ was by Sacks and Brenna[37], who enzymatically cleaved the α-N and analyzed the $\delta^{15}N$ of HIS and the cleaved product via GC/C/IRMS, but no intramolecular $\delta^{15}N_{HIS}$ data for natural materials exist in the literature.

Offline AA purification using liquid chromatography coupled with elemental analyzer-IRMS (EA-IRMS) provides an alternative method by eliminating the need for derivatization. In this approach, underivatized AAs are separated via high-performance liquid chromatography (HPLC), collected in fractions, and analyzed for $\delta^{15}N$ using EA-IRMS[38]. However, EA-IRMS requires significantly larger sample sizes (>3 μmol N per AA) compared to GC/C/IRMS (>5 nmol N) to achieve comparable analytical precision[32], making it less suitable for samples with limited materials. While

nano-scale EA-IRMS (> ~ 35 – 50 nmol N) has been developed[32, 39], it remains uncommon. To the best of our knowledge, only one study has reported $\delta^{15}N_{HIS}$ data of natural samples analyzed using this HPLC/EA-IRMS approach[40].

To overcome these limitations, we present a novel analytical framework for compound-specific and intramolecular δ^{15}N-AA analysis for poly-nitrogenous AAs using HIS as an example. Underivatized HIS is isolated and fraction-collected using ion-exchange chromatography (IC) and separated into two aliquots. One fraction is fully oxidized to NO_3^- using UV-persulfate oxidation for $\delta^{15}N_{HIS\text{-}Total}$ determination, while the other undergoes NaClO oxidation, selectively converting α-N and a portion of sidechain-N to NO_2^- at a known ratio. The δ^{15}N of NO_3^- and NO_2^- products are then analyzed via IRMS to resolve $\delta^{15}N_{HIS\text{-}\alpha}$ and $\delta^{15}N_{HIS\text{-}s}$. We validate this method using seven in-house HIS isotopic standards and five biological samples, assessing its accuracy and precision. This approach provides a robust framework for studying both compound-specific and intramolecular δ^{15}N patterns in poly-nitrogenous AAs (position-specific δ^{15}N for AAs with two N atoms such as Glutamine, tryptophan, and lysine), enabling new insights into nitrogen metabolism and biosynthetic pathways.

2. Experimental Section

2.1 Standard preparation

A working standard solution of histidine (HIS-0) was prepared from a commercial L-histidine powder (VWR, PA, USA) without isotopic enrichment. To generate HIS calibration standards with a wide range of δ^{15}N values, HIS-0 was mixed gravimetrically with isotopically labeled L-histidine monohydrochloride monohydrate standards (Cambridge Isotope, MA, USA) at known proportions. The *α-series* (HIS-*α*1, *α*2, *α*3) was produced by mixing HIS-0 with a labeled L-histidine standard enriched in ^{15}N exclusively at the α-position (98% ^{15}N), while the *w-series* (HIS-w1, w2, w3) was prepared using an L-histidine standard uniformly labeled with 98% ^{15}N at all N positions. The molecular average δ^{15}N of each standard ($\delta^{15}N_{HIS\text{-}Total}$) was determined by elemental analyzer-isotope ratio mass spectrometry (EA-IRMS) at the University of California Davis Stable Isotope Facility. Additionally, a urocanic acid solution was prepared from a commercial powder (Acros, USA) as a structural analog of the HIS imidazole sidechain. This urocanic acid standard was used to evaluate the reactivity and isotopic behavior of sidechain N during subsequent oxidation steps (discussed below).

To evaluate HIS separation from other AAs, seven standard AA mixtures were prepared by combining each HIS isotopic standard (HIS-0, -α1, -α2, -α3, -w1, -w2, -w3) with L-alanine (Ala), L-arginine (Arg), L-asparagine (Asn), D/L-aspartic acid (Asp), L-cysteine (Cys), L-glutamic acid (Glu), L-glutamine (Gln), glycine (Gly), L-isoleucine (Ile), L-leucine (Leu), L-lysine (Lys), D/L-methionine (Met), L-phenylalanine (Phe), D/L-serine (Ser), D/L-threonine (Thr), L-tyrosine (Tyr), and D/L-valine (Val). The final AA concentrations were adjusted to 5 mM for HIS, Asp, Glu, Gln, and Phe, and 2.5 mM for all other AAs.

2.2 Sample Preparation

To further validate the method for natural samples, a suite of materials was analyzed including: 1) a cyanobacteria powder (*Spirulina Pacifica*) that has been used as a multi-lab quality control standard for different CSIA-AA methods[41, 42]. 2) Copepod and euphausiid samples that were collected from the eastern tropical North Pacific (ETNP; 14.02°N, 104.27°W) during the R/V *Sally Ride* (*SR2011*, Scripps Institution of Oceanography) cruise from December 2020 to January 2021

[43]. 3) particulate organic matter (POM) in the size fraction of 0.3 – 53 μm that was collected using a pre-combusted glass fiber filter (GF-75, 0.3 μm pore size) during the same cruise at 35 m depth using a McLane large-volume in-situ filtration system (WTS-LV; McLane Research Laboratories) [44]. 4) A muscle tissue sample from a striped mullet (*Mugil cephalus*) that was collected in Nueces Bay, TX, in 2014. Sample collection details are provided in Supplementary Table ST1.

Extraction of AAs including HIS from natural samples followed previously established protocols (Figure 1)[41, 42, 45, 46]. Briefly, 15–50 mg of dried biological samples or three-quarters of a GF-75 filter were hydrolyzed in 6N HCl at 110°C for 22 hours to release AAs from proteins. This sample mass was chosen to ensure sufficient recovery of HIS, given its relatively low abundance in natural materials. Following hydrolysis, lipids were extracted using n-hexane/dichloromethane (6:5, v/v) and removed from the aqueous hydrolysates containing AAs. The samples were then completely dried at 40°C under vacuum (RapidVap; Labconco) and redissolved in 0.05N HCl. Metal ions were removed via cation-exchange chromatography following previously established protocols[42, 47]. HIS and other AAs were eluted with 10% NH_4OH, dried at 35°C under vacuum, and reconstituted in 0.2–7 mL of Milli-Q water to achieve a target HIS concentration of 2–5 mM before chromatographic separation.

2.3 Ion-Exchange Chromatography separation and collection

HIS was isolated from standard mixtures and natural samples using an ion-exchange chromatography system (ICS 5000+; Thermo Fisher Scientific) equipped with a CarboPac PA10 semi-preparative column (9 × 250 mm, 10 μm particle size, <10 Å pore size). An automated fraction collector (AFC 3000; Thermo Fisher Scientific) received ~90% of the flow, while the rest was directed to a pulse amperometric detector (Thermo Fisher Scientific) for peak detection.

Samples (25 μL of standard mixtures or natural extracts) were injected into the ion-exchange chromatography (IC) system using a mobile phase consisting of (A) Milli-Q water, (B) 1M NaOH, and (C) 1M NaOAc at a flow rate of 5 mL/min. The chromatographic method was optimized for selective HIS separation and collection (Figure 2). An isocratic elution (70% A, 40% B) was applied for the first 33 minutes to achieve effective separation of HIS from other AAs, followed by a gradient elution (40% A, 10% B, 50% C) from 33 to 57 minutes to elute the remaining AAs. The system was re-equilibrated with 70% A and 40% B for 20 minutes before the next injection to ensure consistent performance.

HIS was collected into pre-combusted glass vials, and a procedural blank with an equivalent collection window was included to account for potential isotopic interferences from potential co-eluting nitrogenous compounds that could be oxidized to NO_3^- or NO_2^- during subsequent chemical processing (Figure 2). To assess the reproducibility of the analytical procedure, HIS from each standard mixture was analyzed in triplicate, while HIS from natural samples was analyzed in at least duplicate. HIS concentrations in natural samples were quantified by calibration against a series of standard mixtures. Collected fractions were split into two aliquots (20 – 60 nmol of HIS in each aliquot) for oxidation (UV+POR or NaClO) (Figure 1).

2.4 UV+POR oxidation

For $\delta^{15}N_{HIS\text{-}Total}$ measurement, HIS was fully oxidized to NO_3^- using UV-persulfate oxidation (POR) modified after Foreman et al.[48]. The persulfate reagent (0.185M) was prepared by dissolving 1.25 g of recrystallized potassium persulfate (Fisher Chemical) and 0.4 g of NaOH (semi-conductor grade, Honeywell, NC, USA) in 25 ml of Milli-Q water. Oxidation was performed

in pre-combusted quartz vials (PurQ, Momentive Technologies) containing 10–80 nmol of HIS/ urocanic acid standards or IC-collected fractions (~9.8 mL), with 175 µL of POR reagent added. Samples were sealed with borosilicate stoppers and irradiated for 3 hours in a UV oxidation chamber (7900, Ace Glass) equipped with a 1200-W mercury lamp (7825-40, Ace Glass), allowing the complete conversion of organic N to NO_3^-. Reaction blanks (Milli-Q water) were processed identically. The oxidation yields were verified by quantifying the NO_3^- produced using a nutrient discrete analyzer (AQ300; Seal Analytical; US EPA Method 126-A), and oxidized samples were stored at 4°C before isotope analysis.

2.5 NaClO oxidation

The α-N and a small portion of the side-N of HIS (as determined below) were oxidized to NO_2^- using NaClO with previously established procedures[42, 49]. The catalytic reagent (0.665 g NaBr in 100 mL 10M NaOH) and oxidizing reagent (4.25 mL of 5.25% NaClO diluted to 100 mL) were freshly prepared. Each reaction vial contained 50 nmol of HIS/ urocanic acid standard or IC-collected fractions (~ 3.5 – 10 ml), to which 0.1 mL of catalytic reagent and 0.1 mL of oxidizing reagent were sequentially added. After incubation at 50°C for 30 minutes in a water bath, the reaction was quenched with 0.2 ml of Na_2AsO_2 solution (5.1 g of Na_2AsO_2 in 100 ml of MilliQ water). Triplicate NaClO reaction blanks (Milli-Q water) were processed under identical conditions and included in each sample batch to account for potential background contributions and ensure analytical accuracy. The concentration of the produced NO_2^- was determined using a nutrient discrete analyzer (AQ300; Seal Analytical; US EPA Method 354.1).

2.6 Conversion to N_2O and $\delta^{15}N$ analysis

Reduction of NO_3^- or NO_2^- to N_2O and the subsequent $\delta^{15}N$ analysis was performed at University of Massachusetts Dartmouth (UMD). About 40 nmol of NO_3^- obtained from UV+POR oxidation was reduced to N_2O in serum vials by chemical conversion using Ti (III) following the procedures described in Altabet et al.[50]. To calibrate the unknowns, triplicates of MilliQ water blanks, USGS34, USGS35, and an in-house NO_3^- isotopic reference standard received the same treatment as the samples. Around 10 – 12 nmol of NO_2^- in samples oxidized by NaClO, along with triplicates of MilliQ water blanks and three in-house NO_2^- isotopic reference standards, were converted to N_2O by NaN_3 in serum vials following previously established procedures[42, 49, 51, 52].

$\delta^{15}N$ analysis of N_2O was conducted using a purge-and-trap continuous-flow isotope ratio mass spectrometer (PT/CF/IRMS; Isoprime Ltd) following the established procedures[50]. MilliQ water blanks, and NO_3^- and NO_2^- isotopic reference standards were analyzed at the beginning and end of each sample analysis sequence. The analytical precision of $\delta^{15}N$-N_2O measurement is ± 0.06‰.

2.7 Data correction and calibration

Raw $\delta^{15}N$-N_2O values were first corrected for blank contributions from the Ti (III) or NaN_3 conversion and then calibrated against the isotopic reference standards following the protocol from Altabet et al.[50]. Reaction blank correction was performed using an isotope mass balance equation [42, 51, 53] to obtain $\delta^{15}N$ values for the UV + persulfate oxidation ($\delta^{15}N_{UV+POR}$) and NaClO oxidation ($\delta^{15}N_{ClO}$) of HIS samples:

$$\delta^{15}N_{UV+POR\ or\ ClO} = \frac{\delta^{15}N_s\, A_s - \delta^{15}N_{blk}\, A_{blk}}{A_s - A_{blk}} \qquad (1)$$

where $\delta^{15}N_s$ and A_s represent the measured $\delta^{15}N$ and N content (in nmol) of the HIS samples, and $\delta^{15}N_{blk}$, and A_{blk} correspond to the same parameters for procedural blanks. HIS and urocanic acid

standards directly oxidized by UV + POR or NaClO were corrected using the respective reaction blanks, while IC procedural blanks were used to correct HIS fractions collected from IC separations of both standard mixtures and natural samples.

To generate a calibration curve for $\delta^{15}N_{UV+POR}$, values from pure HIS standards and IC-collected HIS standards were plotted against their independently measured $\delta^{15}N$ values ($\delta^{15}N_{HIS\text{-}Total}$) from EA-IRMS:

$$\delta^{15}N_{UV+POR} = m\,\delta^{15}N_{HIS\text{-}Total} + c \qquad (2)$$

where m and c are the slope and y-intercept of the linear regression model. The $\delta^{15}N_{UV+POR}$ of natural samples were then calibrated using equation (2) to yield $\delta^{15}N_{HIS\text{-}Total}$.

To resolve the $\delta^{15}N$ of α-N ($\delta^{15}N_{HIS\text{-}\alpha}$) and sidechain-N ($\delta^{15}N_{HIS\text{-}s}$, representing the average $\delta^{15}N$ of two imidazole N atoms), the following equations were applied:

$$\delta^{15}N_{ClO} = r\,(\delta^{15}N_{His\text{-}\alpha} + \varepsilon_\alpha) + (1\text{-}r)\,(\delta^{15}N_{His\text{-}s} + \varepsilon_s) \qquad (3)$$

$$\delta^{15}N_{HIS\text{-}Total} = \frac{1}{3}\,\delta^{15}N_{His\text{-}\alpha} + \frac{2}{3}\delta^{15}N_{His\text{-}s} \qquad (4)$$

where ε_α and ε_s represent fractionation factors for NaClO oxidation at the α-N and side-N sites, respectively. Literature values for NaClO oxidation of α-N and imino-N in other AAs range from -2.4‰ to 3.3‰[49]. Based on previous studies, ε_α was assumed to be 0.6‰, corresponding to the fractionation factor for IC-purified phenylalanine (Phe)[42]. Phe was chosen as an analog for estimating the ε_α of HIS due to its similar NaClO oxidation yield (~70%[42]; Supplementary Table ST3) and aromatic sidechain structure[42]. ε_s was obtained by the difference between $\delta^{15}N_{UV+POR}$ and $\delta^{15}N_{ClO}$ of urocanic acid, a structural analog of HIS's sidechain.

The fraction *r*, representing the proportion of NO_2^- derived from α-N oxidation by NaClO reaction, was estimated by plotting $\delta^{15}N_{ClO}$ against $\delta^{15}N_{HIS\text{-}Total}$ for the α-series:

$$\delta^{15}N_{ClO} = m_{\alpha,\,ClO}\,\delta^{15}N_{HIS\text{-}Total} + c_{\alpha,\,ClO} \qquad (5)$$

where $m_{\alpha,\,ClO}$ and $c_{\alpha,\,ClO}$ are the slope and y-intercept, respectively. Since $\delta^{15}N_{HIS\text{-}s}$ remains constant ($\delta^{15}N_{HIS\text{-}s0}$) within the α-series, the only unknown in the equation is *r*. $\delta^{15}N_{HIS\text{-}\alpha}$ in equation (3). By substituting equation (4) into equation (5) to obtain equation (6), and by comparing equation (6) with equation (3), r can be calculated from $m_{\alpha,\,ClO}$ while $c_{\alpha,\,ClO}$ encompasses other constant terms including the $\delta^{15}N_{HIS\text{-}s0}$, ε_α, and ε_s:

$$\delta^{15}N_{ClO} = \frac{m_{a,ClO}}{3}\delta^{15}N_{His\text{-}\alpha} + \frac{2m_{a,ClO}}{3}\,\delta^{15}N_{His\text{-}s0} + c_{\alpha,\,ClO} \qquad (6)$$

$$r = \frac{m_{a,\,ClO}}{3} \qquad (7)$$

$$c_{\alpha,\,ClO} = (1 - 3r)\,\delta^{15}N_{His\text{-}s0} + r\,\varepsilon_\alpha + (1 - r)\,\varepsilon_s \qquad (8)$$

$\delta^{15}N_{HIS\text{-}\alpha}$ and $\delta^{15}N_{HIS\text{-}s}$ could thus be calculated from equations (3) and (4) with $\delta^{15}N_{ClO}$, r ratio, and $\delta^{15}N_{HIS\text{-}Total}$ determined by EA-IRMS or calibrated from $\delta^{15}N_{UV+POR}$:

Uncertainties in $\delta^{15}N_{HIS\text{-}Total}$ and $\delta^{15}N_{ClO}$ were reported as the standard deviation of measurements from replicate IC injections. The uncertainties in $\delta^{15}N_{HIS\text{-}\alpha}$ and $\delta^{15}N_{HIS\text{-}s}$ were propagated from the uncertainties in in $\delta^{15}N_{HIS\text{-}Total}$, $\delta^{15}N_{ClO}$, and r ratio. Additional error contributions from instrument precision, blank corrections, and calibration were also quantified, with details provided in the supplementary information.

3. Results and discussions

3.1 Separation and collection of HIS by IC

Baseline separation of HIS from other AAs in both standard mixtures and copepod samples was achieved using isocratic elution with NaOH and Milli-Q water during the first 33 minutes. The method demonstrated excellent retention time reproducibility, as evidenced by the overlaid chromatograms of replicate injections (Figure 2). The IC method was optimized for HIS separation and collection with a total runtime of 73–77 minutes. This included a 20-minute equilibration phase at the beginning and a 20-minute post-elution column wash with NaOAc to ensure complete removal of residual compounds before the next injection. Key parameters such as injection volume, standard and sample concentrations, and the collection window width were carefully adjusted to ensure sufficient N mass was collected for subsequent UV + POR oxidation and $\delta^{15}N$ analysis. Aliquots of each HIS fraction, along with IC procedural blanks, were directly subjected to UV + POR or NaClO oxidation without additional processing.

3.2 UV+POR oxidation and $\delta^{15}N_{HIS\text{-}Total}$

Accurate determination of $\delta^{15}N_{HIS\text{-}Total}$ without isotopic fractionation requires complete and quantitative oxidation of HIS N to NO_3^-. Persulfate oxidation (POR) is a commonly used method for converting organic N to NO_3^-, but low recoveries (~40–60%) have been reported for certain N-heterocyclic compounds, such as benzotriazole and antipyrine[54, 55]. An alternative approach—UV oxidation with hydrogen peroxide (UV/H_2O_2)—yields higher recoveries (~85–90%) for similar compounds, including HIS and adenosine[48, 56]. To further improve oxidation efficiency, we adopted the recommendation of Bronk et al.[54] to use persulfate as the oxidant in UV oxidation (UV+POR), as persulfate has a higher reduction potential and is more readily activated by UV radiation than peroxide[57]. Compared to POR alone or UV/H_2O_2, UV+POR achieves higher and more consistent recoveries for refractory compounds while also reducing oxidation time[54, 58]. The mole ratio of persulfate to N in the sample typically ranges from 10:1 to 500:1 to ensure complete oxidation[54, 55, 58, 59]. In our protocol, we used a ratio of ~216:1, which was sufficient to fully oxidize HIS.

To evaluate extraneous N introduced during sample preparation and oxidation, we quantified UV reaction blanks and IC procedural blanks. UV reaction blanks primarily reflect background N in the persulfate reagent. To minimize this, $K_2S_2O_8$ was recrystallized three times[60]. The UV procedural blank in Milli-Q water measured 1.5 ± 0.4 µM, comparable to previous studies using POR alone (< 2 µM) and UV/H_2O_2 (~1.2 µM)[54]. IC procedural blanks collected from standard mixture injections exhibited slightly higher N concentrations, averaging 2.3 ± 0.5 µM.

After blank subtraction, oxidation yields of HIS isotopic standards in Milli-Q water and IC-purified HIS fractions from standard mixtures approached 100% following 3 hours of UV exposure (Figure 3, Supplementary Table ST2). These consistently high yields confirm that HIS is quantitatively converted to NO_3^- in both simple (Milli-Q) and IC matrices (NaOH). Correcting $\delta^{15}N$ measurements of HIS isotopic standards with UV procedural blanks and IC-purified HIS fractions with paired IC procedural blanks yielded $\delta^{15}N_{UV+POR}$ values that closely matched $\delta^{15}N_{HIS\text{-}Total}$ values obtained via EA-IRMS (Table 1, Figure 4a, 4b).

Linear regression between $\delta^{15}N_{UV+POR}$ and $\delta^{15}N_{HIS\text{-}Total}$ measured by EA-IRMS produced slopes not significantly different from 1 (HIS standards: 1.00 ± 0.01; IC HIS standard fractions: 0.96 ± 0.01), with small intercepts (HIS standards: -0.78 ± 0.12; IC HIS fractions: 0.65 ± 0.15) and strong

linearity ($R^2 > 0.999$; Figure 4a, 4b). These results confirm that accurate $\delta^{15}N_{HIS\text{-}Total}$ values are obtained when appropriate blank corrections are applied. Furthermore, they demonstrate that UV+POR effectively converts HIS-N to NO_3^- with minimal fractionation, whether or not HIS is first separated via IC.

Measurement precision for $\delta^{15}N_{UV+POR}$ ranged from ±0.1‰ to ±1.2‰. Applying equation (2) for calibration, we determined $\delta^{15}N_{HIS\text{-}Total}$ values for natural samples ranging from 2.5 ± 0.1‰ to 5.2 ± 0.8‰ (Table 2). Propagated error from instrument precision, blank correction, and calibration was generally below 0.2‰ (Supplementary Information), which is lower than the observed standard deviation of replicate $\delta^{15}N_{HIS\text{-}Total}$ measurements (±0.1‰ – 1.3‰). Consequently, the standard deviation of replicates is reported as the uncertainty for $\delta^{15}N_{HIS\text{-}Total}$ in Table 1.

The precision achieved in this study is comparable to $\delta^{15}N_{HIS\text{-}Total}$ uncertainties obtained from GC/C/IRMS for biological samples (±0.4‰ to ±2.6‰)[21, 23, 24] and within the uncertainty range of $\delta^{15}N$ values for other AAs analyzed by CSIA-AA methods (~±0.13‰ to ±1‰)[31, 61]. These findings suggest our method is a reliable approach for determining $\delta^{15}N_{HIS\text{-}Total}$ with high accuracy and precision.

3.3 Estimation of $\delta^{15}N_{HIS\text{-}\alpha}$ and $\delta^{15}N_{HIS\text{-}s}$ with NaClO oxidation

NaClO specifically oxidizes the α-N of AA to NH_3 via Strecker degradation[62], which is then quantitatively converted to NO_2^- under alkaline conditions[49]. The oxidation yield, relative to the initial α-N concentration, was generally ~70–80% for all HIS standards and natural samples (Supplementary Table ST3). The reaction blanks were very low (< 1.3μM), minimizing potential bias in $\delta^{15}N$ measurements. Previous studies have reported that a small fraction of sidechain N from poly-nitrogenous AAs such as HIS, arginine, tryptophan, and asparagine can also be oxidized to NO_2^- during this reaction[49]. In our study, we calculated *r* values (the proportion of NO_2^- originating from α-N oxidation) of ~0.80–0.83 for HIS isotopic standards in Milli-Q water and IC-purified HIS fractions in NaOH, based on the slopes of $\delta^{15}N_{ClO}$ versus $\delta^{15}N_{HIS\text{-}Total}$ in the HIS-α series (Figure 5a, 5b). This indicates that ~17–20% of the NO_2^- product originated from the sidechain-N, which is significantly higher than the oxidation yield of urocanic acid (~3%; Supplementary Table ST2), a structural analog of the HIS sidechain. The enhanced oxidation of HIS sidechain N, compared to urocanic acid, may be attributed to the presence of α-N or the formation of a Strecker aldehyde with an imidazole sidechain during HIS degradation[63]. This likely increases the susceptibility of the sidechain N to oxidation, leading to a higher fraction of sidechain-derived NO_2^- in HIS relative to urocanic acid, which does not form Strecker aldehyde during NaClO oxidation.

Given the observed *r* values for IC-purified HIS fractions, equation (3) can be rewritten as equation (9).

$$\delta^{15}N_{NaClO} = 0.83\ (\delta^{15}N_{His\text{-}\alpha} + \varepsilon_\alpha) + 0.17\ (\delta^{15}N_{His\text{-}s} + \varepsilon_s) \qquad (9)$$

The fractionation factor ε_s for sidechain N was determined as -1.3‰ by subtracting molecular average $\delta^{15}N$ of urocanic acid (3.8 ± 0.8‰, obtained from UV+POR oxidation) from its $\delta^{15}N$ (2.5 ± 0.9‰) obtained by NaClO oxidation. Substituting ε_α = + 0.6‰ and ε_s = -1.3‰ into equation (9), $\delta^{15}N_{HIS\text{-}s}$ and $\delta^{15}N_{HIS\text{-}\alpha}$ could thus be estimated by equations (4) and (9). The combining contribution of ε_α (0.6‰) and ε_s (-1.3‰) to the estimation of $\delta^{15}N_{HIS\text{-}s}$ and $\delta^{15}N_{HIS\text{-}\alpha}$ would be + 0.19‰ only, such that $\delta^{15}N_{HIS\text{-}s}$ and $\delta^{15}N_{HIS\text{-}\alpha}$ would be mostly driven by $\delta^{15}N_{HIS\text{-}Total}$ and $\delta^{15}N_{ClO}$.

The estimated $\delta^{15}N_{HIS-\alpha}$ and $\delta^{15}N_{HIS-s}$ values for HIS isotopic standards are shown in Table 1. The α-series exhibited $\delta^{15}N_{HIS-s}$ values (~ -8 to -9‰) that were indistinguishable from HIS-0, confirming that only the α-N was enriched in ^{15}N. In contrast, the w-series showed increases in both $\delta^{15}N_{HIS-\alpha}$ and $\delta^{15}N_{HIS-s}$, consistent with the isotopic labeling of all N atoms in this series.

The precision of $\delta^{15}N_{ClO}$ measurements in HIS fractions from standard mixtures and natural samples was generally better than ±1.3‰, with most samples showing uncertainties of <±0.7‰. Errors in $\delta^{15}N_{HIS-\alpha}$ and $\delta^{15}N_{HIS-s}$, propagated from uncertainties in $\delta^{15}N_{HIS-Total}$ and $\delta^{15}N_{ClO}$, ranged from ±0.4–1.0‰ for standard mixtures and ±0.5–1.6‰ for most natural samples. The overall precision of $\delta^{15}N_{HIS-\alpha}$ and $\delta^{15}N_{HIS-s}$ measurements obtained in this study is comparable to reported uncertainties in $\delta^{15}N_{HIS-Total}$ for biological samples analyzed using GC/C/IRMS[21, 23, 24]. These results support the reliability of our analytical scheme for distinguishing α- and sidechain N isotopic compositions in HIS.

3.4 Molecular average and intramolecular $\delta^{15}N_{HIS}$ of natural samples

The $\delta^{15}N_{HIS-Total}$ values of natural samples ranged from 2.5 – 5.2‰ (Table 2), consistent with previously reported $\delta^{15}N_{HIS-Total}$ values in biological samples analyzed using GC/C/IRMS (-2.4 – 6.8‰)[21-24]. To provide further context, $\delta^{15}N$ values of the source AA phenylalanine (Phe) and the trophic AA glutamic acid (Glu) were also measured in the same samples using the IC × PT-CF-IRMS method [42]. Across all samples, $\delta^{15}N_{HIS-Total}$ was lower than $\delta^{15}N_{Glu}$ by ~4–16‰ but within ±3‰ of $\delta^{15}N_{Phe}$. This pattern is consistent with previous observations in marine consumers, where $\delta^{15}N_{HIS-Total}$ closely tracks $\delta^{15}N_{Phe}$ (<±5‰) but remains significantly lower than $\delta^{15}N_{Glu}$ (>10‰)[21, 23, 24]. This trend reflects the extensive transamination that enriches Glu in ^{15}N compared to source AAs, particularly with increasing trophic level[7, 45, 64].

Intramolecular $\delta^{15}N$ heterogeneity within HIS molecules was observed in the HIS-0 standard and all biological samples, except for POM (Figure 6, Table 2). The $\Delta\delta^{15}N_{\alpha-s}$ ($\delta^{15}N_{HIS-\alpha} - \delta^{15}N_{HIS-s}$) of HIS-0 was approximately +8‰. This contrasts with the average $\Delta\delta^{15}N_{\alpha-s}$ of -9‰ reported by Sacks and Brenna[37] for commercial HIS standards from four different vendors (Acros, Belgium; Avocado Organics, UK; J.T. Baker, USA; Sigma, USA), which were analyzed by enzymatic cleavage of α-N followed by GC/C/IRMS. Commercial L-histidine is typically produced via microbial fermentation[65], meaning it retains a biological isotopic signature. The opposing $\Delta\delta^{15}N_{\alpha-s}$ sign in our HIS-0 standard may be caused by the differences in manufacturing processes of HIS adopted by different vendors. However, the consistent observation of positive $\Delta\delta^{15}N_{\alpha-s}$ across biological samples in this study suggests a systematic isotopic fractionation pattern related to N metabolism.

The cyanobacteria sample, a primary producer capable of HIS biosynthesis, exhibited a positive $\Delta\delta^{15}N_{\alpha-s}$ of +2.8‰. This suggests that the relatively ^{15}N-enriched α-N may come from Glu, which typically has higher $\delta^{15}N$ than sidechain N due to extensive transamination during AA biosynthesis. POM in the surface ocean primarily consists of phytoplankton, heterotrophic bacteria, and detrital organic matter. The small $\Delta\delta^{15}N_{\alpha-s}$ in POM (-1.1‰) may result from an integration of biosynthetic signals from different microbial sources and isotopic fractionation during environmental degradation. Compared to cyanobacteria and POM, the three consumer samples exhibited markedly higher $\Delta\delta^{15}N_{\alpha-s}$ values (fish: +12.6‰, copepods and euphausiids: +23 to +25‰; Table 2, Figure 6), with $\delta^{15}N_{HIS-\alpha}$ values elevated relative to $\delta^{15}N_{Phe}$ and approaching $\delta^{15}N_{Glu}$. The substantial ^{15}N enrichment of α-N in consumers is surprising given the limited exchange between HIS α-N and the metabolic N pool. Since higher trophic organisms cannot synthesize HIS de novo,

it is unlikely that metabolic N directly contributes to HIS formation or to the ^{15}N enrichment of α-N. One potential metabolic pathway of HIS involves its reversible conversion to imidazole pyruvate and another AA by donating the α-N to a keto acid[66] (Supplementary Figure 1b). However, the enzyme responsible for imidazole pyruvate production exhibits low activity under physiological conditions[66-68]. Therefore, HIS in consumers should not directly exchange α-N with other AAs, making it unlikely that $\delta^{15}N_{HIS\text{-}\alpha}$ tightly coupled with $\delta^{15}N_{Glu}$ or the $\delta^{15}N$ of the metabolic N pool.

Instead, we hypothesize that $\delta^{15}N_{HIS\text{-}\alpha}$ in consumers is influenced by dietary inputs and the extent of HIS catabolism. The N isotopic fractionation associated with histidase-mediated deamination of HIS has not been directly studied, but similar ammonia-lyases that cleave α-N of Phe preferentially remove ^{14}N, leading to ^{15}N enrichment in the residual Phe[69]. If HIS deamination follows this pattern, it would increase $\delta^{15}N_{HIS\text{-}\alpha}$ while having minimal effect on $\delta^{15}N_{HIS\text{-}s}$, as the sidechain N does not participate in deamination. HIS catabolism rates are linked to physiological and environmental factors such as starvation and N limitation, both of which can decrease HIS concentrations in diatom and fish[70, 71]. Additionally, N isotopic turnover and HIS catabolism rates are typically higher in organs than in muscle tissues[70, 72]. Thus, interspecies differences in $\Delta\delta^{15}N_{\alpha\text{-}s}$ among the consumers may reflect variations in diet quality, growth stage, physiological status, protein turnover rates, and tissue type[73-76]. Notably, the strong ^{15}N enrichment in consumer α-N of HIS has not been previously identified because the $\delta^{15}N_{HIS\text{-}\alpha}$ signal is diluted by lower $\delta^{15}N_{HIS\text{-}s}$ values, resulting in $\delta^{15}N_{HIS\text{-}Total}$ values that remain comparable to $\delta^{15}N_{Phe}$.

The trophic transfer of $\delta^{15}N_{HIS}$ at both molecular average and intramolecular levels within a local planktonic food web can be inferred by comparing the omnivorous copepods and carnivorous euphausiids collected from the same location (Supplementary Table ST1). Euphausiids acquire HIS from copepods or other shared food sources. The nearly identical $\delta^{15}N_{HIS\text{-}\alpha}$ and $\delta^{15}N_{HIS\text{-}s}$ values between these two taxa suggest that intramolecular $\delta^{15}N$ distribution in HIS remains largely unaltered during trophic transfer. Future controlled feeding experiments across different taxonomic groups will provide further insight into how $\delta^{15}N_{HIS\text{-}\alpha}$ and $\delta^{15}N_{HIS\text{-}s}$ change with dietary inputs and metabolic processes.

3.5 Summary

This study validates an analytical framework for measuring $\delta^{15}N$ values of poly-nitrogenous amino acids at both compound-specific and intramolecular levels, using histidine as a model. We demonstrated that UV+POR oxidation efficiently converts HIS to NO_3^- in various matrices, including Milli-Q water and NaOH. This approach can be extended to other poly-nitrogenous AAs, provided they are baseline-separated and fully oxidized to NO_3^- by UV+POR. When combined with NaClO oxidation, which selectively targets α-N, our approach will enable intramolecular $\delta^{15}N$ analysis of poly-N AAs such as arginine, glutamine, asparagine, lysine, and tryptophan.

The analytical techniques and instrumentation used in this approach are widely available, making the method readily adoptable by many laboratories. For example, conversion of NO_3^- or NO_2^- to N_2O for $\delta^{15}N$ analysis is routinely performed in commercial and research facilities using well-established methods, including Cd/azide reduction[51], the bacterial denitrifier method[77], and Ti(III) reduction[50].

Beyond its utility in food web studies, where differential trophic ^{15}N enrichment among AAs helps infer trophic relationships, intramolecular $\delta^{15}N$ analysis of poly-N AAs provides valuable insights into nitrogen metabolism and biochemical pathways. Potential applications include tracing

nucleobase synthesis from the amide-N of glutamine[78], investigating the role of arginine's guanidino-N in the urea cycle[79], and examining the formation of indole during tryptophan biosynthesis—a signaling molecule that regulates many physiological functions[80, 81].

Supporting Information

The Supporting Information is available in the following files:

Supplementary Table ST1-3 and Supplementary Figure SF1 (PDF)

Supplementary information: Error analysis and propagation (PDF)

Acknowledgement

This work was funded by NSF grants (OCE 1829947, 1829834, 2216356, 2242041, and 2242042).

Author Contributions

All authors have given approval to the final version of the manuscript.

Notes

The authors declare no conflict of interests.

Table of Contents Graphic

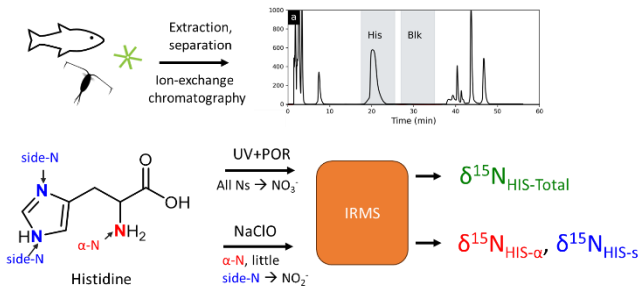

Figures and Tables

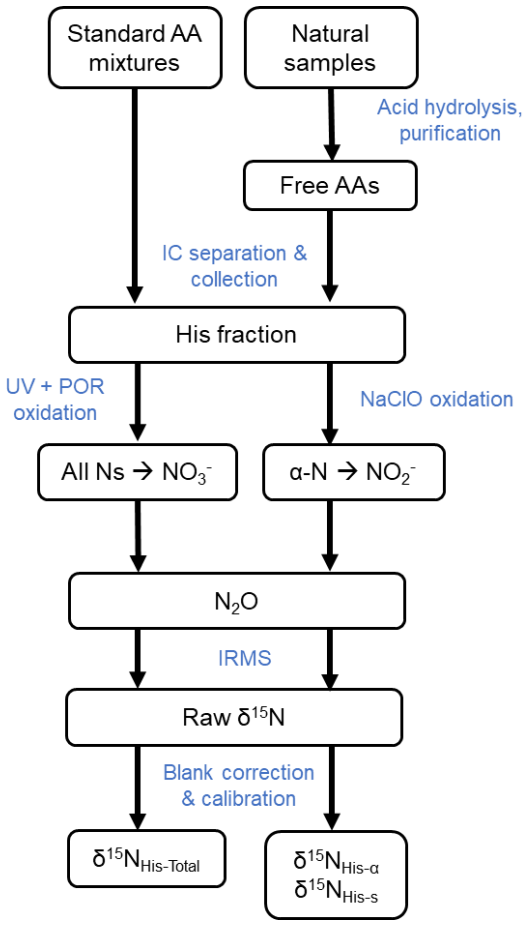

Figure 1. Procedural flowchart of $\delta^{15}N_{HIS}$ analysis of standards and biological samples.

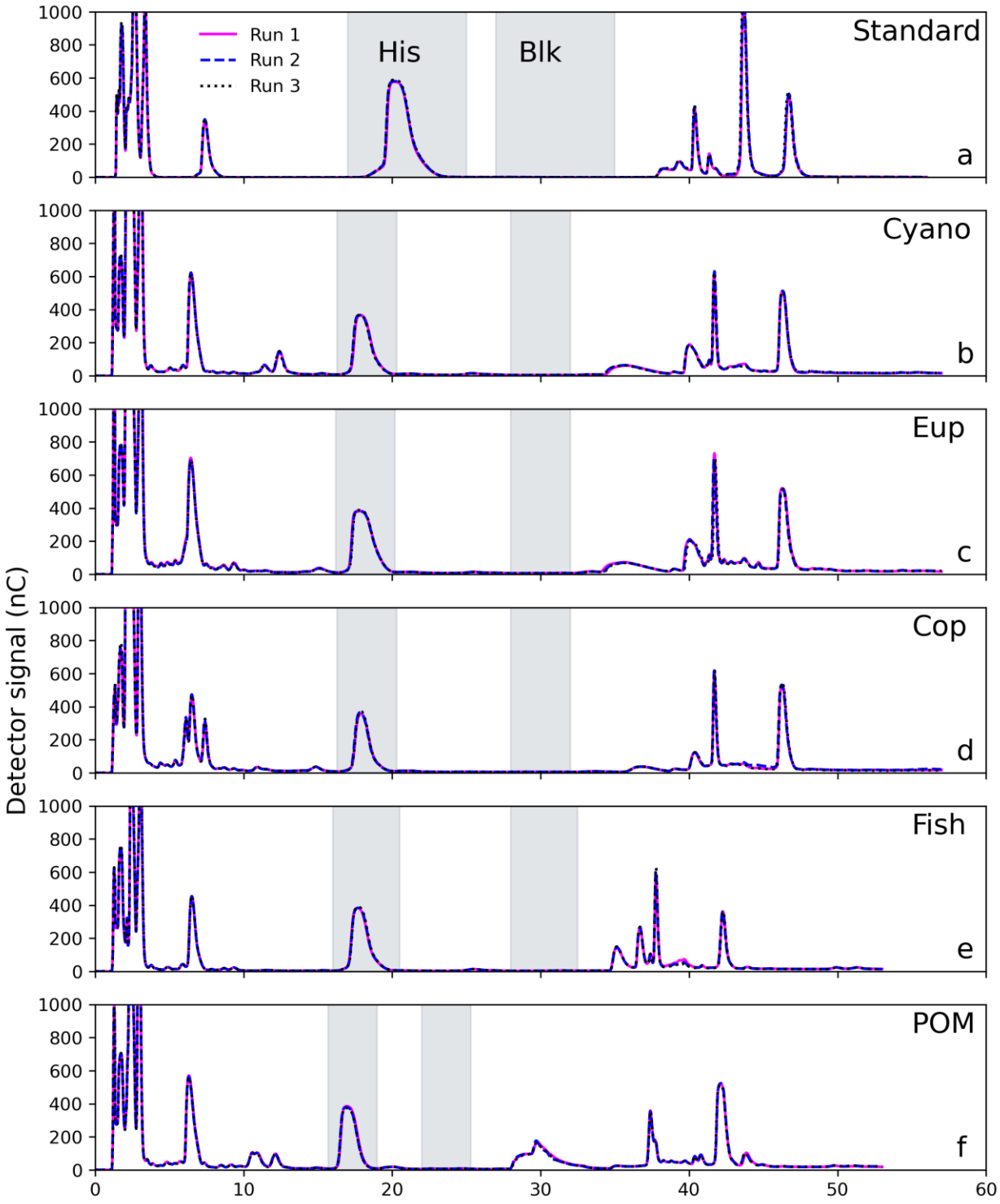

Figure 2. IC chromatograms of (a) standard mixture; (b) cyanobacteria; (c) euphausiid; (d) copepod; (e) fish; and (f) POM. Replicate injections were overlaid. The shaded areas denote the fraction collection windows of HIS and blank.

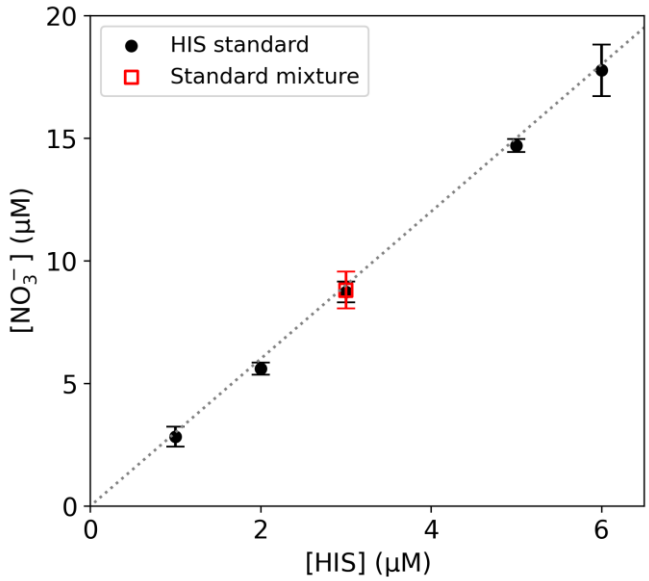

Figure 3. The concentration of NO_3^- yielded from UV + POR oxidation on HIS isotopic standards in various concentrations and IC HIS fractions collected from injections of standard mixtures. The dotted line indicates the 100% yield with a ratio of 3:1 for [NO_3^-]:[HIS].

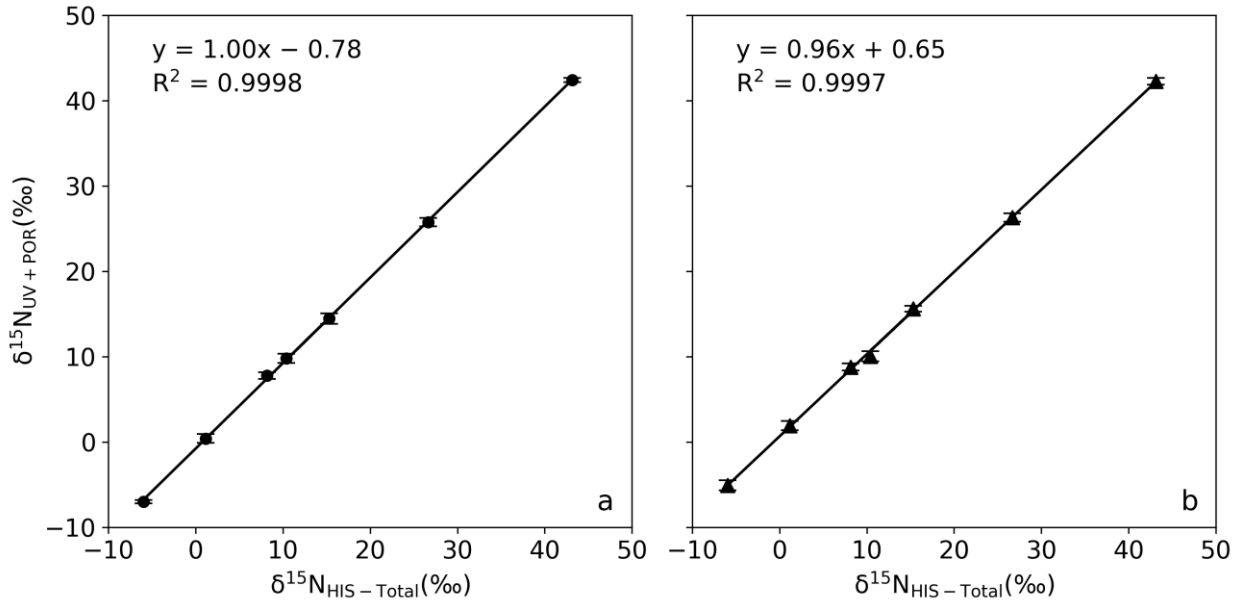

Figure 4. $\delta^{15}N_{UV+POR}$ of (a) HIS isotopic standards and (b) IC HIS fractions collected from injections of standard mixtures are plotted against their $\delta^{15}N_{HIS-Total}$ values determined by EA-IRMS listed in Table 1. Slopes of both series are close to 1 (HIS standards: 1.00 ± 0.01; IC HIS standard fractions: 0.96 ± 0.01) with small intercepts (HIS standards: -0.78 ± 0.12; IC HIS fractions: 0.65 ± 0.15). Error bars are generally smaller than the symbols.

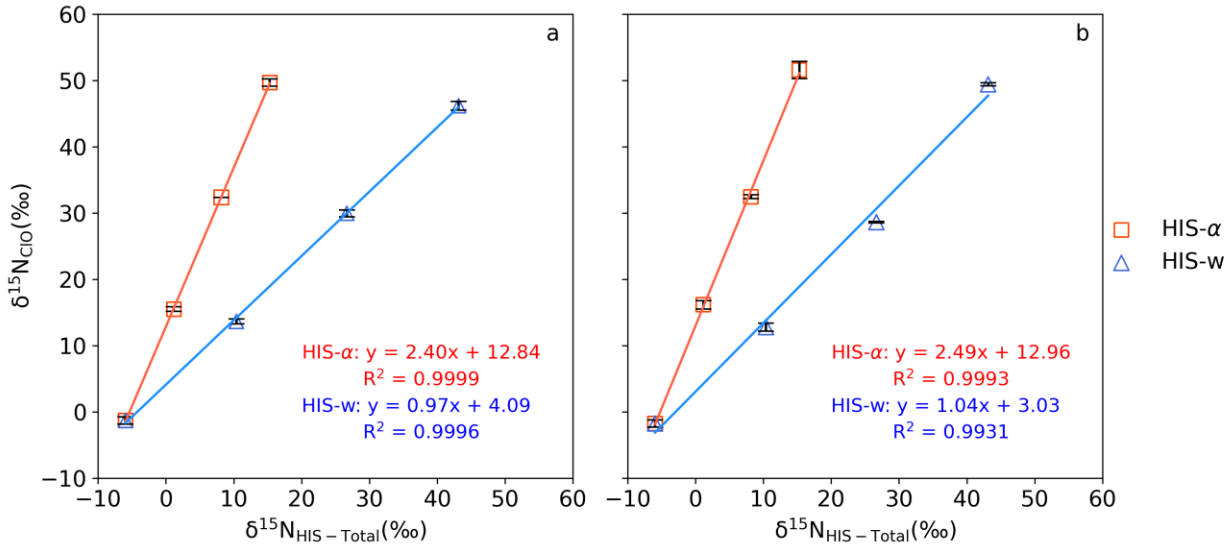

Figure 5. $\delta^{15}N_{ClO}$ of (a) HIS isotopic standards and (b) IC HIS fractions collected from injections of standard mixtures are plotted against their $\delta^{15}N_{EA}$ values listed in Table 1. Error bars are generally smaller than the symbols. The slopes of the α-series are used for calculating the r ratio.

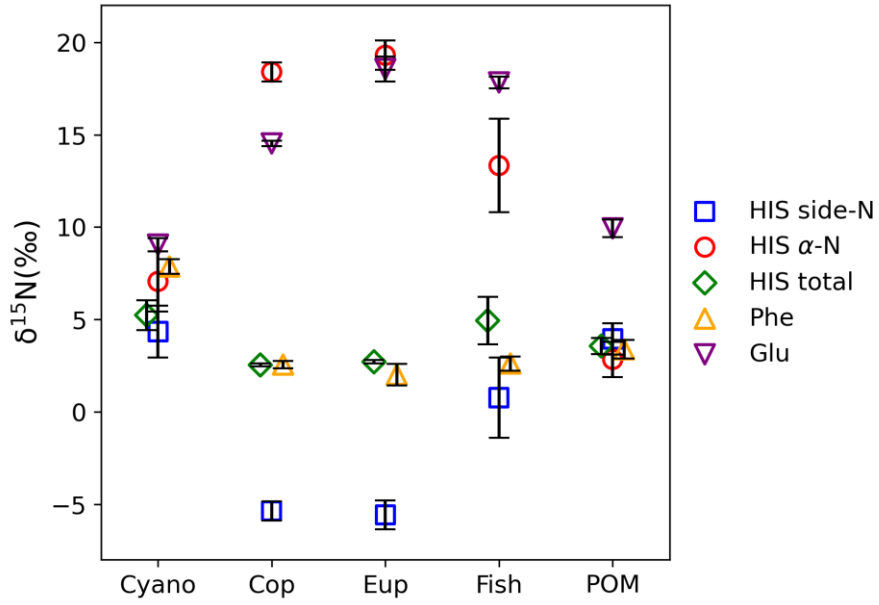

Figure 6. $\delta^{15}N$ of α-N and side-N of natural samples calculated from $\delta^{15}N_{UV+POR}$ (calibrated to $\delta^{15}N_{HIS\text{-}Total}$) and $\delta^{15}N_{ClO}$ of IC-collected HIS fractions. $\delta^{15}N_{Phe}$ and $\delta^{15}N_{Glu}$ are included for comparison.

Standard	HIS standards in H2O				IC-Collected HIS fractions		
	$\delta^{15}N_{HIS\text{-}Total}$ (‰)	$\delta^{15}N_{ClO}$ (‰)	$\delta^{15}N_{HIS\text{-}s}$ (‰)	$\delta^{15}N_{HIS\text{-}\alpha}$ (‰)	$\delta^{15}N_{ClO}$ (‰)	$\delta^{15}N_{HIS\text{-}s}$ (‰)	$\delta^{15}N_{HIS\text{-}\alpha}$ (‰)
His-0	-6.0 ± 0.0	-1.3 ± 0.6	-9.1 ± 0.5	0.3 ± 0.5	-1.8 ± 0.6	-8.6 ± 0.5	-0.7 ± 0.5
His-a1	1.2 ± 0.0	15.5 ± 0.3	-8.9 ± 0.4	21.3 ± 0.4	16.2 ± 0.6	-8.7 ± 0.6	20.9 ± 0.6
His-a2	8.2 ± 0.1	32.3 ± 0.0	-8.9 ± 0.4	42.4 ± 0.4	32.4 ± 0.3	-7.9 ± 0.5	40.3 ± 0.5
His-a3	15.3 ± 0.0	49.7 ± 0.5	-9.1 ± 0.6	64.1 ± 0.6	51.5 ± 1.3	-8.8 ± 1.1	63.5 ± 1.1
His-w1	10.4 ± 0.0	13.6 ± 0.4	8.3 ± 0.4	14.7 ± 0.4	12.8 ± 0.6	9.0 ± 0.5	13.2 ± 0.5
His-w2	26.7 ± 0.1	29.9 ± 0.5	24.5 ± 0.5	31.0 ± 0.5	28.6 ± 0.1	25.6 ± 0.4	28.8 ± 0.4
His-w3	43.1 ± 0.0	46.2 ± 0.6	41.2 ± 0.6	47.1 ± 0.6	49.4 ± 0.2	39.2 ± 0.4	51.1 ± 0.4

Table 1. $\delta^{15}N$ of α-N and side-N of HIS isotopic standards calculated from $\delta^{15}N_{ClO}$ of IC-collected HIS fractions and $\delta^{15}N_{HIS\text{-}Total}$ determined by EA-IRMS.

Sample	$\delta^{15}N_{HIS\text{-}Total}$ (‰)	$\delta^{15}N_{ClO}$ (‰)	$\delta^{15}N_{HIS\text{-}s}$ (‰)	$\delta^{15}N_{HIS\text{-}\alpha}$ (‰)	$\delta^{15}N_{Phe}$ (‰)	$\delta^{15}N_{Glu}$ (‰)
Cyanobacteria	5.2 ± 0.8	6.9 ± 0.2	4.3 ± 1.4	7.1 ± 1.6	7.9 ± 0.4	9.0 ± 0.4
Copepod	2.5 ± 0.1	14.6 ± 0.5	-5.4 ± 0.5	18.4 ± 0.5	2.6 ± 0.2	14.5 ± 0.1
Euphausiid	2.7 ± 0.1	15.3 ± 1.0	-5.6 ± 0.8	19.3 ± 0.8	2.0 ± 0.6	18.6 ± 0.7
Fish	4.9 ± 1.3	11.5 ± 0.3	0.8 ± 2.2	13.3 ± 2.5	2.6 ± 0.4	17.8 ± 0.3
POM	3.6 ± 0.4	3.3 ± 0.3	3.9 ± 0.8	2.8 ± 0.9	3.4 ± 0.5	9.9 ± 0.5

Table 2. $\delta^{15}N_{HIS}$-α and $\delta^{15}N_{HIS}$-s of natural samples calculated from $\delta^{15}N_{UV+POR}$ (calibrated to $\delta^{15}N_{HIS\text{-}Total}$) and $\delta^{15}N_{ClO}$ of IC-collected HIS fractions. $\delta^{15}N_{Phe}$ and $\delta^{15}N_{Glu}$ were analyzed with the method described by Zhang et al.[42].

References

1. Macko, S. A.; Fogel, M. L.; Hare, P. E.; Hoering, T. C., Isotopic fractionation of nitrogen and carbon in the synthesis of amino acids by microorganisms. *Chemical Geology: Isotope Geoscience section* **1987,** *65* (1), 79-92. DOI:10.1016/0168-9622(87)90064-9

2. Chikaraishi, Y.; Steffan, S. A.; Ogawa, N. O.; Ishikawa, N. F.; Sasaki, Y.; Tsuchiya, M.; Ohkouchi, N., High-resolution food webs based on nitrogen isotopic composition of amino acids. *Ecol. Evol.* **2014,** *4* (12), 2423-2449. DOI:10.1002/ece3.1103

3. McCarthy, M. D.; Lehman, J.; Kudela, R., Compound-specific amino acid δ15N patterns in marine algae: Tracer potential for cyanobacterial vs. eukaryotic organic nitrogen sources in the ocean. *Geochim. Cosmochim. Acta* **2013,** *103*, 104-120. DOI:10.1016/j.gca.2012.10.037

4. Mompeán, C.; Bode, A.; Gier, E.; McCarthy, M. D., Bulk vs. amino acid stable N isotope estimations of metabolic status and contributions of nitrogen fixation to size-fractionated zooplankton biomass in the subtropical N Atlantic. *Deep Sea Res., Part I* **2016,** *114*, 137-148. DOI:10.1016/j.dsr.2016.05.005

5. McMahon, K. W.; McCarthy, M. D., Embracing variability in amino acid δ15N fractionation: mechanisms, implications, and applications for trophic ecology. *Ecosphere* **2016,** *7* (12), e01511. DOI:10.1002/ecs2.1511

6. Vokhshoori, N. L.; McCarthy, M. D.; Close, H. G.; Demopoulos, A. W. J.; Prouty, N. G., New geochemical tools for investigating resource and energy functions at deep-sea cold seeps using amino acid δ15N in chemosymbiotic mussels (Bathymodiolus childressi). *Geobiology* **2021,** *19* (6), 601-617. DOI:10.1111/gbi.12458

7. Ohkouchi, N.; Takano, Y., Organic Nitrogen: Sources, Fates, and Chemistry. **2014**, 251-289. DOI:10.1016/b978-0-08-095975-7.01015-9

8. Ohkouchi, N.; Chikaraishi, Y.; Close, H. G.; Fry, B.; Larsen, T.; Madigan, D. J.; McCarthy, M. D.; McMahon, K. W.; Nagata, T.; Naito, Y. I.; Ogawa, N. O.; Popp, B. N.; Steffan, S.; Takano, Y.; Tayasu, I.; Wyatt, A. S. J.; Yamaguchi, Y. T.; Yokoyama, Y., Advances in the application of amino acid nitrogen isotopic analysis in ecological and biogeochemical studies. *Org. Geochem.* **2017,** *113*, 150-174. DOI:10.1016/j.orggeochem.2017.07.009

9. Abe, H., Role of histidine-related compounds as intracellular proton buffering constituents in vertebrate muscle. *Biochemistry (Mosc.)* **2000,** *65* (7), 757-65.

10. Olson, J. S.; Mathews, A. J.; Rohlfs, R. J.; Springer, B. A.; Egeberg, K. D.; Sligar, S. G.; Tame, J.; Renaud, J.-P.; Nagai, K., The role of the distal histidine in myoglobin and haemoglobin. *Nature* **1988,** *336* (6196), 265-266. DOI:10.1038/336265a0

11. Krämer, U.; Cotter-Howells, J. D.; Charnock, J. M.; Baker, A. J. M.; Smith, J. A. C., Free histidine as a metal chelator in plants that accumulate nickel. *Nature* **1996,** *379* (6566), 635-638. DOI:10.1038/379635a0

12. Schneider, F., Histidine in Enzyme Active Centers. *Angewandte Chemie International Edition in English* **1978,** *17* (8), 583-592. DOI:10.1002/anie.197805831

13. Kinuta, M.; Ubuka, T.; Yao, W. B.; Zhao, Y. Q.; Shimizu, H., Isolation of S-[2-carboxy-1-(1H-imidazol-4-yl)ethyl]-3-thiolactic acid, a new metabolite of histidine, from normal human urine and its formation from S-[2-carboxy-1-(1H-imidazol-4-yl)ethyl]cysteine. *Biochem. J.* **1994,** *297* (3), 475-478. DOI:10.1042/bj2970475

14. Boldyrev, A. A.; Aldini, G.; Derave, W., Physiology and Pathophysiology of Carnosine. *Physiol. Rev.* **2013,** *93* (4), 1803-1845. DOI:10.1152/physrev.00039.2012

15. Baslow, M. H., Function of theN-acetyl-l-histidine system in the vertebrate eye. *J. Mol. Neurosci.* **1998,** *10* (3), 193-208. DOI:10.1007/BF02761774

16. Alifano, P.; Fani, R.; Liò, P.; Lazcano, A.; Bazzicalupo, M.; Carlomagno, M. S.; Bruni, C. B., Histidine biosynthetic pathway and genes: structure, regulation, and evolution. *Microbiol. Rev.* **1996,** *60* (1), 44-69. DOI:10.1128/mr.60.1.44-69.1996

17. Stepansky, A.; Leustek, T., Histidine biosynthesis in plants. *Amino Acids* **2006,** *30* (2), 127-142. DOI:10.1007/s00726-005-0247-0

18. O'Connell, T. C., 'Trophic' and 'source' amino acids in trophic estimation: a likely metabolic explanation. *Oecologia* **2017,** *184* (2), 317-326. DOI:10.1007/s00442-017-3881-9

19. Aqvist, S. E. G., Amino acid interrelationships during growth, studied with N15-labeled glycine in regenerating rat liver. *Acta Chemica Scandinavica* **1951,** *5*, 1065–1073.

20. Metges, C. C.; Petzke, K.-J.; Hennig, U., Gas Chromatography/Combustion/Isotope Ratio Mass Spectrometric Comparison of N -Acetyl- and N-Pivaloyl Amino Acid Esters to Measure 15N Isotopic Abundances in Physiological Samples: A Pilot Study on Amino Acid Synthesis in the Upper Gastro-intestinal Tract of Minipigs. *J. Mass Spectrom.* **1996,** *31* (4), 367-376. DOI:10.1002/(SICI)1096-9888(199604)31:4<367::AID-JMS310>3.0.CO;2-V

21. Lorrain, A.; Graham, B.; Ménard, F.; Popp, B.; Bouillon, S.; Van Breugel, P.; Cherel, Y., Nitrogen and carbon isotope values of individual amino acids: a tool to study foraging ecology of penguins in the Southern Ocean. *Mar. Ecol. Progr. Series* **2009,** *391*, 293-306. DOI:10.3354/meps08215

22. Petzke, K. J.; Boeing, H.; Klaus, S.; Metges, C. C., Carbon and Nitrogen Stable Isotopic Composition of Hair Protein and Amino Acids Can Be Used as Biomarkers for Animal-Derived Dietary Protein Intake in Humans12. *The Journal of Nutrition* **2005,** *135* (6), 1515-1520. DOI:10.1093/jn/135.6.1515

23. Popp, B. N.; Graham, B. S.; Olson, R. J.; Hannides, C. C. S.; Lott, M. J.; López-Ibarra, G. A.; Galván-Magaña, F.; Fry, B., Insight into the Trophic Ecology of Yellowfin Tuna, Thunnus albacares, from Compound-Specific Nitrogen Isotope Analysis of Proteinaceous Amino Acids. *Terrestrial Ecology* **2007,** *1*, 173-190. DOI:10.1016/s1936-7961(07)01012-3

24. Schmidt, K.; Atkinson, A.; Petzke, K.-J.; Voss, M.; Pond, D. W., Protozoans as a food source for Antarctic krill, Euphausia superba: Complementary insights from stomach content, fatty acids, and stable isotopes. *Limnol. and Oceanogr.* **2006,** *51* (5), 2409-2427. DOI:10.4319/lo.2006.51.5.2409

25. Brenner, M.; Ames, B. N., The Histidine Operon and Its Regulation. In *Metabolic Regulation (Third Edition)*, Vogel, H. J., Ed. Academic Press: 1971; pp 349-387.

26. Yamaguchi, Y. T.; Chikaraishi, Y.; Takano, Y.; Ogawa, N. O.; Imachi, H.; Yokoyama, Y.; Ohkouchi, N., Fractionation of nitrogen isotopes during amino acid metabolism in heterotrophic and chemolithoautotrophic microbes across Eukarya, Bacteria, and Archaea: Effects of nitrogen sources and metabolic pathways. *Org. Geochem.* **2017,** *111*, 101-112. DOI:10.1016/j.orggeochem.2017.04.004

27. Bender Robert, A., Regulation of the Histidine Utilization (Hut) System in Bacteria. *Microbiol. Mol. Biol. Rev.* **2012,** *76* (3), 565-584. DOI:10.1128/mmbr.00014-12

28. Polkinghorne, M. A.; Hynes, M. J., L-histidine utilization in Aspergillus nidulans. *J. Bacteriol.* **1982,** *149* (3), 931-940. DOI:10.1128/jb.149.3.931-940.1982

29. Hofmann, D.; Gehre, M.; Jung, K., Sample preparation techniques for the determination of natural 15N/14N variations in amino acids by gas chromatography-combustion-isotope ratio mass spectrometry (GC-C-IRMS). *Isot. Environ. Health Stud.* **2003,** *39* (3), 233-244. DOI:10.1080/1025601031000147630

30. Hušek, P.; Macek, K., Gas chromatography of amino acids. *J. Chromatogr. A* **1975,** *113* (2), 139-230. DOI:10.1016/S0021-9673(00)86962-9

31. Ishikawa, N. F.; Itahashi, Y.; Blattmann, T. M.; Takano, Y.; Ogawa, N. O.; Yamane, M.; Yokoyama, Y.; Nagata, T.; Yoneda, M.; Haghipour, N.; Eglinton, T. I.; Ohkouchi, N., Improved Method for Isolation and Purification of Underivatized Amino Acids for Radiocarbon Analysis. *Anal. Chem.* **2018,** *90* (20), 12035-12041. DOI:10.1021/acs.analchem.8b02693

32. Ishikawa, N. F.; Ogawa, N. O.; Sun, Y.; Chikaraishi, Y.; Takano, Y.; Ohkouchi, N., Integrative assessment of amino acid nitrogen isotopic composition in biological tissue samples determined by GC/C/IRMS, LC × EA/IRMS, and LC × GC/C/IRMS. *Limnol. Oceanogr. Methods* **2022,** *20* (9), 531-542. DOI:10.1002/lom3.10502

33. Walsh, R. G.; He, S.; Yarnes, C. T., Compound-specific δ13C and δ15N analysis of amino acids: a rapid, chloroformate-based method for ecological studies. *Rapid Commun. Mass Spectrom.* **2014,** *28* (1), 96-108. DOI:10.1002/rcm.6761

34. Silverman, S. N.; Phillips, A. A.; Weiss, G. M.; Wilkes, E. B.; Eiler, J. M.; Sessions, A. L., Practical considerations for amino acid isotope analysis. *Org. Geochem.* **2022,** *164*, 104345. DOI:10.1016/j.orggeochem.2021.104345

35. Huang, Z. H.; Wang, J.; Gage, D. A.; Watson, J. T.; Sweeley, C. C.; Husek, P., Characterization of N-ethoxycarbonyl ethyl esters of amino acids by mass spectrometry. *J. Chromatogr.* **1993,** *635* (2), 271-281. DOI:10.1016/0021-9673(93)80370-n

36. Kheirbeik, L.; Hatté, C.; Balesdent, J., Labelled microbial culture as a calibration medium for 13C-isotope measurement of derivatized compounds: application to tert-butyldimethylsilyl amino acids. *Rapid Commun. Mass Spectrom.* **2016,** *30* (18), 1991-2001. DOI:10.1002/rcm.7678

37. Sacks, G. L.; Brenna, J. T., 15N/14N Position-Specific Isotopic Analyses of Polynitrogenous Amino Acids. *Anal. Chem.* **2005,** *77* (4), 1013-1019. DOI:10.1021/ac048903o

38. Broek, T. A. B.; Walker, B. D.; Andreasen, D. H.; McCarthy, M. D., High-precision measurement of phenylalanine δ15N values for environmental samples: A new approach coupling high-pressure liquid chromatography purification and elemental analyzer isotope ratio mass spectrometry. *Rapid Commun. Mass Spectrom.* **2013,** *27* (21), 2327-2337. DOI:10.1002/rcm.6695

39. Swalethorp, R.; Aluwihare, L.; Thompson, A. R.; Ohman, M. D.; Landry, M. R., Errors associated with compound-specific δN analysis of amino acids in preserved fish samples purified by high-pressure liquid chromatography. *Limnol. Oceanogr. Methods* **2020,** *18* (6), 259-270. DOI:10.1002/lom3.10359

40. Sun, Y.; Ogawa, N. O.; Ishikawa, N. F.; Blattmann, T. M.; Takano, Y.; Ohkouchi, N., Application of a porous graphitic carbon column to carbon and nitrogen isotope analysis of underivatized individual amino acids using high-performance liquid chromatography coupled with elemental analyzer/isotope ratio mass spectrometry. *Rapid Commun. Mass Spectrom.* **2023,** *37* (17), e9602. DOI:10.1002/rcm.9602

41. Broek, T. A. B.; McCarthy, M. D., A new approach to δ15N compound-specific amino acid trophic position measurements: preparative high pressure liquid chromatography technique for purifying underivatized amino acids for stable isotope analysis. *Limnol. Oceanogr. Methods* **2014,** *12* (12), 840-852. DOI:10.4319/lom.2014.12.840

42. Zhang, L.; Lee, W.-m.; Kreider-Mueller, A.; Kuhnel, E.; Baca, J.; Ji, C.; Altabet, M., High-precision measurement of phenylalanine and glutamic acid δ15N by coupling ion-exchange chromatography and purge-and-trap continuous-flow isotope ratio mass spectrometry. *Rapid Commun. Mass Spectrom.* **2021,** *35* (13), e9085. DOI:10.1002/rcm.9085

43. Sánchez-Velasco, L.; García-De León, F. J.; Ruvalcada-Aroche, E. D.; Beier, E.; Godínez, V. M.; Jiménez-Rosenberg, S. P. A.; Sánchez-Pérez, E. D.; Contreras-Catala, F.; Mnich, A.; Verma, N.;

Altabet, M., Vertical distribution of zooplankton groups, with an emphasis on fish larvae, in the oxygen minimum zone off southern México (December 2020). *J. Mar. Sys.* **2022,** *236*, 103801. DOI:10.1016/j.jmarsys.2022.103801

44. Lee, C. W. M.; Altabet, M.; Mnich, A.; Zhang, L., Using δ15N of Amino Acids and Nitrate to Investigate Particle Production and Transformation in the Ocean: A Case Study From the Eastern Tropical North Pacific Oxygen Deficient Zone. *Global Biogeochem. Cycles* **2025,** *39* (1), e2024GB008280. DOI:10.1029/2024GB008280

45. Chikaraishi, Y.; Ogawa, N. O.; Kashiyama, Y.; Takano, Y.; Suga, H.; Tomitani, A.; Miyashita, H.; Kitazato, H.; Ohkouchi, N., Determination of aquatic food-web structure based on compound-specific nitrogen isotopic composition of amino acids. *Limnol. Oceanogr. Methods* **2009,** *7* (11), 740-750. DOI:10.4319/lom.2009.7.740

46. McCarthy, M. D.; Benner, R.; Lee, C.; Fogel, M. L., Amino acid nitrogen isotopic fractionation patterns as indicators of heterotrophy in plankton, particulate, and dissolved organic matter. *Geochim.Cosmochim. Acta* **2007,** *71* (19), 4727-4744. DOI:10.1016/j.gca.2007.06.061

47. Takano, Y.; Kashiyama, Y.; Ogawa, N. O.; Chikaraishi, Y.; Ohkouchi, N., Isolation and desalting with cation-exchange chromatography for compound-specific nitrogen isotope analysis of amino acids: application to biogeochemical samples. *Rapid Commun. Mass Spectrom.* **2010,** *24* (16), 2317-2323. DOI:10.1002/rcm.4651

48. Foreman, R. K.; Björkman, K. M.; Carlson, C. A.; Opalk, K.; Karl, D. M., Improved ultraviolet photo-oxidation system yields estimates for deep-sea dissolved organic nitrogen and phosphorus. *Limnol. Oceanogr. Methods* **2019,** *17* (4), 277-291. DOI:10.1002/lom3.10312

49. Zhang, L.; Altabet, M. A., Amino-group-specific natural abundance nitrogen isotope ratio analysis in amino acids. *Rapid Commun. Mass Spectrom.* **2008,** *22* (4), 559-566. DOI:10.1002/rcm.3393

50. Altabet, M. A.; Wassenaar, L. I.; Douence, C.; Roy, R., A Ti(III) reduction method for one-step conversion of seawater and freshwater nitrate into N2O for stable isotopic analysis of 15N/14N, 18O/16O and 17O/16O. *Rapid Commun. Mass Spectrom.* **2019,** *33* (15), 1227-1239. DOI:10.1002/rcm.8454

51. McIlvin, M. R.; Altabet, M. A., Chemical Conversion of Nitrate and Nitrite to Nitrous Oxide for Nitrogen and Oxygen Isotopic Analysis in Freshwater and Seawater. *Anal. Chem.* **2005,** *77* (17), 5589-5595. DOI:https://10.1021/ac050528s

52. Zhang, L.; Altabet, M. A.; Wu, T.; Hadas, O., Sensitive Measurement of NH4+ 15N/14N (δ15NH4+) at Natural Abundance Levels in Fresh and Saltwaters. *Anal. Chem.* **2007,** *79* (14), 5297-5303. DOI:https://10.1021/ac070106d

53. Polissar, P. J.; Fulton, J. M.; Junium, C. K.; Turich, C. C.; Freeman, K. H., Measurement of 13C and 15N Isotopic Composition on Nanomolar Quantities of C and N. *Anal. Chem.* **2009,** *81* (2), 755-763. DOI:10.1021/ac801370c

54. Bronk, D. A.; Lomas, M. W.; Glibert, P. M.; Schukert, K. J.; Sanderson, M. P., Total dissolved nitrogen analysis: comparisons between the persulfate, UV and high temperature oxidation methods. *Mar. Chem.* **2000,** *69* (1), 163-178. DOI:10.1016/S0304-4203(99)00103-6

55. Nydahl, F., On the peroxodisulphate oxidation of total nitrogen in waters to nitrate. *Water Research* **1978,** *12* (12), 1123-1130. DOI:10.1016/0043-1354(78)90060-X

56. Walsh, T. W., Total dissolved nitrogen in seawater: a new-high-temperature combustion method and a comparison with photo-oxidation. *Mar. Chem.* **1989,** *26* (4), 295-311. DOI:10.1016/0304-4203(89)90036-4

57. Yang, Q.; Ma, Y.; Chen, F.; Yao, F.; Sun, J.; Wang, S.; Yi, K.; Hou, L.; Li, X.; Wang, D., Recent advances in photo-activated sulfate radical-advanced oxidation process (SR-AOP) for refractory organic pollutants removal in water. *Chem. Eng. J.* **2019,** *378*, 122149. DOI:10.1016/j.cej.2019.122149

58. Yang, S.; Wang, P.; Yang, X.; Shan, L.; Zhang, W.; Shao, X.; Niu, R., Degradation efficiencies of azo dye Acid Orange 7 by the interaction of heat, UV and anions with common oxidants: Persulfate, peroxymonosulfate and hydrogen peroxide. *J. Hazard. Mater.* **2010,** *179* (1), 552-558. DOI:10.1016/j.jhazmat.2010.03.039

59. Knapp, A. N.; Sigman, D. M.; Lipschultz, F., N isotopic composition of dissolved organic nitrogen and nitrate at the Bermuda Atlantic Time-series Study site. *Global Biogeochem. Cycles* **2005,** *19* (1), DOI:10.1029/2004gb002320

60. Solórzano, L.; Sharp, J. H., Determination of total dissolved nitrogen in natural waters. *Limnol. Oceanogr.* **1980,** *25* (4), 751-754. DOI:10.4319/lo.1980.25.4.0751

61. Yarnes, C. T.; Herszage, J., The relative influence of derivatization and normalization procedures on the compound-specific stable isotope analysis of nitrogen in amino acids. *Rapid Commun. Mass Spectrom.* **2017,** *31* (8), 693-704. DOI:10.1002/rcm.7832

62. Schonberg, A.; Moubacher, R., The Strecker Degradation of α-Amino Acids. *Chem. Rev.* **1952,** *50* (2), 261-277. DOI:10.1021/cr60156a002

63. Zamora, R.; Delgado, R. M.; Hidalgo, F. J., Strecker aldehydes and α-keto acids, produced by carbonyl–amine reactions, contribute to the formation of acrylamide. *Food Chem.* **2011,** *128* (2), 465-470. DOI:10.1016/j.foodchem.2011.03.054

64. McClelland, J. W.; Montoya, J. P., Trophic relationships and the nitrogen isotopic composition of amino acids in plankton *Ecology* **2002,** *83* (8), 2173-2180. DOI:10.1890/0012-9658(2002)083[2173:TRATNI]2.0.CO;2

65. Becker, J.; Wittmann, C., Bio-based production of chemicals, materials and fuels – Corynebacterium glutamicum as versatile cell factory. *Curr. Opin. Biotechnol.* **2012,** *23* (4), 631-640. DOI:10.1016/j.copbio.2011.11.012

66. Coote, J. G.; Hassall, H., The degradation of l-histidine, imidazolyl-l-lactate and imidazolylpropionate by Pseudomonas testosteroni. *Biochem. J.* **1973,** *132* (3), 409-422. DOI:10.1042/bj1320409

67. Hacking, A. J.; Hassall, H., The purification and properties of l-histidine-2-oxoglutarate aminotransferase from Pseudomonas testosteroni. *Biochem. J.* **1975,** *147* (2), 327-334. DOI:10.1042/bj1470327

68. Noguchi, T.; Okuno, E.; Minatogawa, Y.; Kido, R., Purification, characterization and identification of rat liver histidine-pyruvate aminotransferase isoenzymes. *Biochem.J.* **1976,** *155* (1), 107-115. DOI:10.1042/bj1550107

69. Hermes, J. D.; Weiss, P. M.; Cleland, W. W., Use of nitrogen-15 and deuterium isotope effects to determine the chemical mechanism of phenylalanine ammonia-lyase. *Biochem.* **1985,** *24* (12), 2959-2967. DOI:10.1021/bi00333a023

70. Abe, H.; Brill, R. W.; Hochachka, P. W., Metabolism of L-Histidine, Carnosine, and Anserine in Skipjack Tuna. *Physiol. Zool.* **1986,** *59* (4), 439-450. DOI:10.1086/physzool.59.4.30158597

71. Pan, Y.; Hu, F.; Yu, C.; Li, C.; Huang, T.; Hu, H., Amino Acid Catabolism During Nitrogen Limitation in Phaeodactylum tricornutum. *Front. Plant Sci.* **2020,** *11*, DOI:10.3389/fpls.2020.589026

72. Madigan, D. J.; Litvin, S. Y.; Popp, B. N.; Carlisle, A. B.; Farwell, C. J.; Block, B. A., Tissue Turnover Rates and Isotopic Trophic Discrimination Factors in the Endothermic Teleost, Pacific Bluefin Tuna (Thunnus orientalis). *PLoS One* **2012,** *7* (11), e49220. DOI:10.1371/journal.pone.0049220

73. Bradley, C. J.; Madigan, D. J.; Block, B. A.; Popp, B. N., Amino Acid Isotope Incorporation and Enrichment Factors in Pacific Bluefin Tuna, Thunnus orientalis. *PLoS One* **2014,** *9* (1), e85818. DOI:10.1371/journal.pone.0085818

74. Conceição, L. E. C.; van der Meeren, T.; Verreth, J. A. J.; Evjen, M. S.; Houlihan, D. F.; Fyhn, H. J., Amino acid metabolism and protein turnover in larval turbot (Scophthalmus maximus) fed natural zooplankton or Artemia. *Mar. Biol.* **1997,** *129* (2), 255-265. DOI:10.1007/s002270050166

75. Kaushik, S. J.; Seiliez, I., Protein and amino acid nutrition and metabolism in fish: current knowledge and future needs. *Aquacult. Res.* **2010,** *41* (3), 322-332. DOI:10.1111/j.1365-2109.2009.02174.x

76. Ventura, M.; Catalan, J., Variability in amino acid composition of alpine crustacean zooplankton and its relationship with nitrogen-15 fractionation. *J. Plankton Res.* **2010,** *32* (11), 1583-1597. DOI:10.1093/plankt/fbq066

77. McIlvin, M. R.; Casciotti, K. L., Technical updates to the bacterial method for nitrate isotopic analyses. *Anal. Chem.* **2011,** *83* (5), 1850-1856.

78. Koga, T.; Takano, Y.; Ogawa, N. O.; Hollingsworth, E. H.; Oba, Y.; Ohkouchi, N., Compound-Specific Carbon and Nitrogen Isotopic Analyses of Underivatized Pyrimidine and Purine Nucleobases. *ACS Earth and Space Chem.* **2025**, DOI:10.1021/acsearthspacechem.4c00110

79. Kendall, I. P.; Evershed, R. P., Determination of Arginine δ15N Values in Plant and Animal Proteins by Gas Chromatography–Combustion–Isotope Ratio Mass Spectrometry. *Anal. Chem.* **2020,** *92* (19), 13246-13253. DOI:10.1021/acs.analchem.0c02438

80. Fiore, A.; Murray, P. J., Tryptophan and indole metabolism in immune regulation. *Curr. Opin. Immunol.* **2021,** *70*, 7-14. DOI:10.1016/j.coi.2020.12.001

81. Palego, L.; Betti, L.; Rossi, A.; Giannaccini, G., Tryptophan Biochemistry: Structural, Nutritional, Metabolic, and Medical Aspects in Humans. *J. Amino Acids* **2016,** *2016* (1), 8952520. DOI:10.1155/2016/8952520